An Ankyrin-related Gene (*unc-44*) Is Necessary for Proper Axonal Guidance in *Caenorhabditis elegans*

Anthony J. Otsuka,*‡ Rodrigo Franco,‡ Bin Yang,* Kyu-Hwan Shim,* Lan Zhao Tang,* Yu Yong Zhang,* Pratumtip Boontrakulpoontawee,* Ayyamperumal Jeyaprakash,‡ Edward Hedgecock,§ Virginia I. Wheaton,‡ and Alan Sobery*

*Department of Biological Sciences, 4120 Illinois State University, Normal, Illinois 61790-4120; ‡Department of Genetics, University of California, Berkeley, California 94720; and §Department of Biology, Johns Hopkins University, Baltimore, Maryland 21218

Abstract. *Caenorhabditis elegans unc-44* mutations result in aberrant axon guidance and fasciculation with inappropriate partners. The *unc-44* gene was cloned by transposon tagging, and verified by genetic and molecular analyses of six transposon-induced alleles and their revertants. Nucleotide sequence analyses demonstrated that *unc-44* encodes a series of putative ankyrin-related proteins, including AO49 ankyrin (1815 aa, 198.8 kD), AO66 ankyrin (1867 aa, 204 kD), and AO13 ankyrin (≤4700 aa, ≤517 kD). In addition to the major set of ~6 kb alternatively spliced transcripts, minor transcripts were observed at ~3, 5, 7, and 14 kb. Evidence is provided that mutations in the ~14-kb AO13 ankyrin transcript are responsible for the neuronal defects. These molecular studies provide the first evidence that ankyrin-related molecules are required for axonal guidance.

ALTHOUGH the molecular basis of neural development has been the object of intense study in recent years, the detailed mechanisms of axon guidance remain unknown (for general reviews see Dodd and Jessell, 1988; Jessell, 1988; Takeichi, 1988; Sanes, 1989; Takeichi, 1991; Rathjen et al., 1992; Gumbiner, 1993; for *C. elegans* reviews see Hedgecock et al., 1987; Wadsworth and Hedgecock, 1992).

Mutations in the *unc-44* gene affect the direction of axonal outgrowth for many axons (Hedgecock et al., 1985; Siddiqui, 1990; Siddiqui and Culotti, 1991; McIntire et al., 1992), including the postdeirid (PDE)[1] axon, which normally extends from the postdeirid sensillum on the lateral surface of the nematode to the ventral nerve cord (White et al., 1986). In *unc-44* mutants, the initial direction of PDE axon outgrowth along the basement membrane is apparently random, and the misdirected PDE axon fasciculates with inappropriate partners (Hedgecock et al., 1985).

The discovery that the *C. elegans unc-6* gene encodes a laminin B chain-related product provided evidence that directed axonal outgrowth and cell migration require interactions with the extracellular matrix (Hedgecock et al., 1990), and that these interactions use laminin or related proteins in both invertebrates and vertebrates (Jessell, 1988; Sanes, 1989; Hedgecock et al., 1990; Serafini et al., 1994). The product of the *unc-5* gene, which affects dorsalward cell migrations and axon outgrowth, has been proposed to be a cell surface protein which may interact with the extracellular matrix (Leung-Hagesteijn et al., 1992). Thus, it was likely that other mutations affecting axonal outgrowth and guidance were defects in cytoskeletal or extracellular matrix structures. The actin/α-actinin framework of growth cone filopodia or the spectrin/ankyrin network underlying the cytoplasmic surface of the plasma membrane could be the targets for mutations affecting axon outgrowth and growth cone adhesion. In this study, we have discovered that the wild-type *unc-44* gene, which is required for proper axonal guidance, encodes a series of putative ankyrin-related proteins.

Ankyrin (or bands 2.1 and 2.2) has been most thoroughly studied in erythrocyte "ghosts" (for reviews see Lazarides and Woods, 1989; Bennett, 1990; Bennett, 1992; Michaely and Bennett, 1992; Lambert and Bennett, 1993; Peters and Lux, 1993). In erythrocytes, ankyrin monomers anchor the spectrin network to the transmembrane anion exchanger (AE1 or band 3). The AE1-binding domain can also bind to tubulin, microtubules, and intermediate filaments (Georgatos et al., 1987). Ankyrin is composed of three domains: (*1*) a membrane protein-binding domain containing 23

Address all correspondence to A. Otsuka, Department of Biological Sciences, 4120 Illinois State University, Normal, IL 61790-4120. Tel.: (309) 438-5220. Fax: (309) 438-3722.

The current address of Dr. Franco is Wyeth-Ayerst Research, CN8000, Princeton, NJ 08543-8000.

The current address of Dr. Jeyaprakash is Entomology and Nematology Department, Institute of Food and Agricultural Sciences, University of Florida, Bldg. 970, Hull Road, P. O. Box 110620, Gainesville, FL 32611-0620.

1. *Abbreviations used in this paper*: AE1, anion exchanger 1; PDE, postdeirid; RBC, red blood cell.

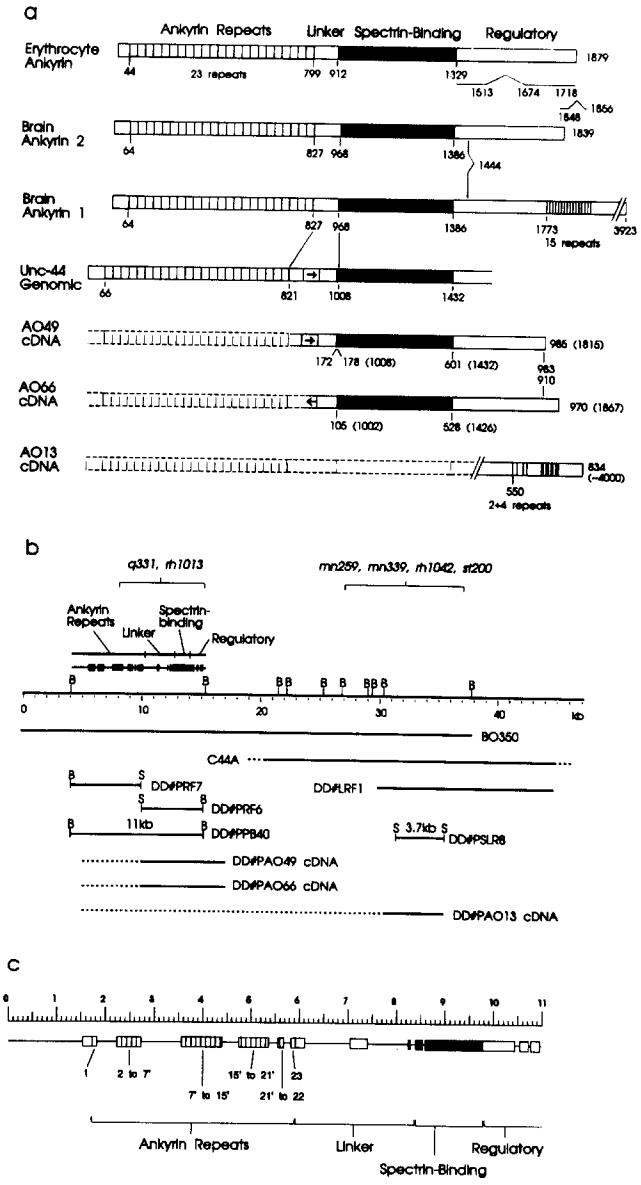

Figure 1. (*a*) The proposed structures of ankyrin-related proteins. Multiple proposed forms of human erythrocyte ankyrin (Lambert et al., 1990; Lux et al., 1990), human brain ankyrin 2, a partial structure of brain ankyrin 1 (Otto et al., 1991), and partial structures of the putative nematode *unc-44* ankyrin-related products are shown. Brain ankyrins 1 and 2 contain different carboxyl termini produced by alternative splicing at aa position 1444 (Otto et al., 1991). In brain ankyrin 1, alternative splicing results in insertion of 2085 aa, including 15 repeats of a 12-aa sequence, into the carboxyl-terminal domain to produce a 440-kD product (Kunimoto et al., 1991, Chan et al., 1993). For *unc-44*, the amino acids are numbered from the start of the partial cDNAs, while those expected in the full-length protein are noted in parentheses. In the *unc-44* products, alternative splicing modifies the carboxyl terminus (at cDNA aa positions 983 and 910) in a manner similar to that found in erythrocyte ankyrin. In the linker domain, between the ankyrin repeats and the spectrin-binding domain, the DD#PAO49 product contains a 6-aa alternatively spliced microexon relative to DD #PAO66. An inversion of the nucleic acid sequence (*boxed arrow*) occurs in the linker domain in the DD#AO66 cDNA clone. The ankyrin repeat domains shown as dashed lines are those expected on the basis of Northern blot analysis. (*b*) Map of the *unc-44* region. The positions and extents of the cosmid (BO350 and C44A), phage (DD#LRF1), genomic plasmid subclones (DD#PRF6, DD #PRF7, DD#PPB40, and DD#PSLR8), and cDNA clones (DD#PAO 13, DD#PAO49, and DD#PAO66) are displayed. The positions of *unc-44* mutations are shown above the genomic map. The ankyrin domains present on the 11-kb BamHI fragment in DD #PPB40 are shown along with the exon map (*filled blocks*) above the genomic map. Relevant restriction sites for BamHI (*B*) and SalI (*S*) are noted. The dashed lines extending from the cDNA clones estimate the full extent of the RNAs as determined by Northern blot analysis. The cDNA clones were obtained by screening cDNA libraries with probes corresponding to DD#PPB40 (11 kb) and DD#PSLR8 (3.7 kb). The dashed lines extending from cosmid clone C44A represent the uncertainty of nematode DNA junctions in the clone. (*c*) The genomic organization of the 11-kb BamHI fragment. The 11-kb region from DD#PPB40 was sequenced by the exonuclease III deletion method using the subclones DD#PRF6 and DD#PRF7. The exons are represented by boxes and the introns by a line. The ankyrin repeats subdivide the boxes and the strong spectrin-binding domain similarity is shown in black. The primed numbers represent breaks within the individual ankyrin repeats.

~33-amino acid repeats (ankyrin repeats), (*2*) a spectrin-binding domain, and (*3*) a regulatory domain (Wallin et al., 1984; Weaver and Marchesi, 1984; Weaver et al., 1984; Hall and Bennett, 1987; Davis and Bennett, 1990; Lambert et al., 1990; Lux et al., 1990). In this report, the sequence heterogeneity between the vertebrate ankyrins and the *unc-44* products defines an additional "linker" domain between the ankyrin repeat and spectrin-binding domains (see Fig. 1 *a*; see also Platt et al., 1993).

Ankyrin is found in a number of tissues, including the brain (Drenckhahn and Bennett, 1987). Molecular analysis of human brain ankyrin cDNA clones reveals several alternatively spliced RNAs (Otto et al., 1991). The predicted products of two of the RNAs are brain ankyrin 2 (202 kD) with a gross structural similarity to erythrocyte ankyrin, and brain ankyrin 1 (~440 kD) which contains the typical ankyrin repeat, linker, and spectrin-binding domains, but has an extensive carboxyl-terminal domain (Otto et al., 1991; Chan et al., 1993). Brain and erythrocyte ankyrins bind to distinct sites on kidney membranes, suggesting different transmembrane protein targets for the different ankyrins (Davis et al., 1989). Recently, it was demonstrated that ankyrin binds a protein related to the neurofascin cell adhesion molecule in the rat brain (Davis et al., 1993). Thus, ankyrin may interact with other proteins, including cell surface receptors, localizing them on the cell surface.

A minor form of ankyrin (band 2.2), which results from an alternative splicing event that removes a 16-kD polypeptide region from within the regulatory domain, is permanently "activated" to allow enhanced binding to membrane-associated sites (Hall and Bennett, 1987; Davis et al., 1992). In addition, calpain proteolysis of the AE1-binding domain decreases ankyrin binding to AE1 (Hall and Bennett, 1987). Altering the binding affinity of ankyrin for its substrates may allow cytoskeletal remodeling during cell growth and locomotion (Hall and Bennett, 1987).

In previous studies, *unc-44* mutations were isolated in a high level transposition background in order to tag the gene

with transposons (Otsuka et al., 1987). In this paper, we report the molecular cloning and characterization of the *unc-44* gene. The DNA sequence analysis, Southern and Northern blot analysis, and genetic complementation tests demonstrate that the *unc-44* gene has been cloned. Analysis of six spontaneous *unc-44* alleles ascertained that all were due to DNA insertions (see Fig. 1 *b*). Reversions of these six alleles result in in-frame deletions of the transposons or secondary insertions of transposons at RNA splicing junctions.

The composite structures of the *unc-44* ankyrins have been obtained from a combination of cloned genomic and cDNA sequences. These studies demonstrate that alternative splicing produces several transcripts from a single ankyrin-related gene. There is a major set of 6 kb transcripts and several minor transcripts. Paralleling the human *ANK2* gene, *unc-44* encodes "conventional" ankyrin isoforms (AO49 and AO66 ankyrins) with gross similarities to erythrocyte ankyrin and brain ankyrin 2, as well as a much larger form of ankyrin (AO13 ankyrin). Although AO13 ankyrin is predicted to be similar in size to vertebrate brain ankyrin 1, its carboxyl-terminal domain sequence is highly acidic and distinct from that reported from brain ankyrin 1 (Chan et al., 1993).

Materials and Methods

Cloned DNAs and Nematode Strains

Nematode strains and recombinant DNA clones are listed in Table I. The insertion mutations define a single complementation group because they fail to complement in all combinations tested, i.e., the *rh1013* allele failed to complement both *q331* and *rh1042* mutations, while the *q331* allele failed to complement the *rh1042* allele.

Preparation of DNA

Nematodes were cultured and DNA prepared as described previously (Brenner, 1974; Sulston and Brenner, 1974). Plasmid and phage DNAs were prepared by standard methods (Maniatis et al., 1982).

Southern Blot Hybridization

3 μg of each restriction enzyme-digested DNA were fractionated on Tris-borate 0.7% agarose gels containing ethidium bromide, and Southern blots were prepared (Maniatis et al., 1982). After prehybridizing the nitrocellulose filters (Schleicher and Schuell, Inc., Keene, NH), the hybridization was performed in 6× SSC, 0.01 M EDTA, 5× Denhardt's solution, 0.5% SDS, 100 μg of denatured herring sperm DNA/ml, and 1 μg ^{32}P-labeled probe (10^7 cpm/μg), for 12–16 h at 68°C. The blots were washed extensively in 2× SSC and 0.5% SDS at 68°C. The Tc*1* probe was the plasmid pCe2003 (Emmons and Yesner, 1984).

Northern Blot Analysis

RNA was prepared from a mixed-stage population of N2 worms by French pressure cell disruption, lysis with a Polytron homogenizer, or grinding in liquid nitrogen in the presence of guanidinium chloride, followed by selective ethanol precipitation (MacLeod et al., 1981). Messenger RNA was purified on an oligodeoxythymidylic acid-cellulose column (Aviv and Leder, 1972). 5 μg of poly A selected or 20 μg of total nematode RNA were separated on denaturing formaldehyde agarose gels (Lehrach et al., 1977) and analyzed by Northern blot hybridization using Zetaprobe charged nylon membranes (BioRad Laboratories, Richmond, CA) and [α-^{32}P] UTP-labeled riboprobes (5 × 10^7 cpm, 200 Ci/mmol of nucleotide) transcribed from cDNA clones (DD#PAO13, DD#PAO49, and DD#PAO66) or ankyrin repeat (DD#PLT1840) plasmids using a T3/T7 RNA polymerase transcription kit (Stratagene, Inc., La Jolla, CA). The hybridization conditions (manufacturer recommended buffer including 5× SSC, 42°C) and washing conditions (0.1× SSC plus 0.1% SDS, 68°C) were those recommended by Stratagene.

Screening Clone Banks

Six genomic clones were obtained from a phage bank probed by standard methods (Maniatis et al., 1982). Five independent cDNA clones were obtained from ~1.4 million phage of the Barstead-Waterston bank without additional amplification (Barstead and Waterston, 1989).

DNA Sequencing and Computer Analysis

DNA was subcloned into pTZ18R, pTZ19R (Pharmacia LKB Biotechnology, Piscataway, NJ), or pBluescript SK(−) (Stratagene) and sequenced by the dideoxynucleotide method (Sanger et al., 1977). Appropriate subclones were obtained by using suitable restriction fragments or by the exonuclease III deletion method (Henikoff, 1984). DNA sequence was obtained from both DNA strands except in some of the introns. Sequences determined from a single strand were done at least four times. Additional analysis was done using the Pustell and MacVector DNA Sequence Analysis Programs (Eastman Kodak Co., New Haven, CT) and our own programs.

Results

Cloning the unc-44 Gene

To identify a restriction fragment length polymorphism associated with the *unc-44* gene, a set of recombinants was constructed in the *unc-44* region (Table I). Linkage of a Tc*1* transposon to the *unc-44* gene was demonstrated by the presence of a 12.6-kb Tc*1*-containing EcoRI fragment in the *rh1042* mutant and in recombinants retaining the *unc-44 (rh1042)* allele (Fig. 2, lanes *2* and *4*). The wild-type N2 strain and recombinants that have lost the *rh1042* mutant phenotype do not contain this fragment (Fig. 2, lanes *1*, *5*, and *6*). Because the wild-type DNA does not contain a transposon insertion in *unc-44*, no *unc-44*–specific band appears in Fig. 2, lane *1*. However, wild-type DNA did contain an 11-kb fragment when probed with an *unc-44*–specific probe (data not shown). In the *rh1042* revertant, the characteristic 12.6-kb mutant fragment is missing and is replaced by a 14.2-kb fragment (Fig. 2, lane *3*), due to the insertion of a second Tc*1* element. Reversion of transposon-induced mutations by insertion of additional transposons has been described previously (Mount et al., 1988).

EcoRI-cleaved *rh1042* DNA fragments in the 12.6-kb size range were cloned into the EMBL3 bacteriophage lambda vector, and the resulting library was screened with a Tc*1* probe to yield clone DD#LRF7 (Table I). The region flanking the Tc*1* element was subcloned into a plasmid vector and used to screen a wild-type nematode genomic library in EMBL3. Six *unc-44* clones were obtained (Table I) and used to identify cosmid clones (Table I and Fig. 1 *b*).

Southern Blot Analysis of unc-44 DNA Insertion Mutations

To unambiguously demonstrate that the *unc-44* gene had been cloned, six putative transposon-induced mutations and their revertants (Table I) were analyzed by Southern blot hybridization with *unc-44*–specific probes and the results are summarized in Fig. 1 *b*. By Southern analysis with BamHI, EcoRI, PstI, or SalI, and by polymerase chain reaction amplification, the *q331* and *rh1013* mutations were found to be Tc*1* insertions toward the 5′-end of the gene, and their revertants were Tc*1* excisions which restore the *unc-44* reading frame. The *rh1042*, *mn259*, *mn339*, and *st200* mutations were DNA insertions toward the 3′-end of the gene. The

rh1042 allele is a Tc*1* insertion within the DD#PAO13 open reading frame. The six insertion mutations and their in-frame excision in *mn259, q331,* and *rh1013* revertants provide proof that the *unc-44* gene has been cloned. The revertants of *rh1042* and *st200* are secondary Tc*1* insertions at RNA splicing junctions and presumably restore gene activity by altering RNA splicing.

Cloning of cDNAs

To clone cDNAs corresponding to the regions surrounding the *unc-44* DNA insertions, two genomic DNA fragments were used to probe nematode cDNA libraries: (*1*) the 11-kb genomic BamHI fragment flanking the Tc*1* insertions in *q331* and *rh1013* toward the 5′-end of the gene (corresponding to clone DD#PPB40 in Fig. 1 *b*), and (*2*) the 3.7-kb SalI fragment flanking the Tc*1* insertion in *rh1042* toward the 3′-end of the gene (corresponding to DD#PSLR8 in Fig. 1 *b*). DNA sequencing was performed on two clones, DD#PAO49 and DD#PAO66, obtained with the 11-kb probe, and one (DD #PAO13) of the three independent clones with identical restriction patterns obtained with the 3.7-kb probe.

The Ankyrin Repeats Are Grouped into Six Clusters

The overall structure of the AO49 and AO66 ankyrin isoforms (Fig. 3) can be inferred from the domains present on the 11-kb BamHI genomic (DD#PPB40) and the cDNA

Table 1. Nematode Strains and Cloned DNAs

Strain	Genotype	Relevant properties	Source of reference
N2	wild-type	Bristol strain	Brenner, 1974
NJ82	wild-type	Bristol/Bergerac hybrid	Otsuka et al., 1987
RW7097	*mut-6* (*st702*)	High transposition	Mori et al., 1988
TR679	*mut-2* (*r459*)	High transposition	Collins et al., 1987
unc-44 (*rh1013*) derivatives			
NJ94	*unc-44* (*rh1013*)	Sp. mut. from NJ82	Otsuka et al., 1987
NJ280	*unc-44* (*rh1013*10*), *bli-6* (*sc16*)	Double mut.	This work
DD196	*unc-44* (*rh1013*10*), *bli-6* (+)	Unc-44 from NJ280	This work
NJ101	*unc-44* (*rh1013*1*) *rev-1*	Sp. rev.	This work
NJ105	*unc-44* (*rh1013*) *rev-2*	Sp. rev.	This work
unc-44 (*rh1042*) derivatives			
NJ401	*unc-44* (*rh1042*4*)	Sp. mut. from RW7097	This work
NJ441	*unc-44* (*rh1042*8*)	Outcrossed 8x	This work
NJ416	*unc-44* (*rh1042*3*) *bli-6* (*sc16*)	Unc-44 Bli	This work
NJ417	*unc-44* (+), *bli-6* (*sc16*)	Non-Unc Bli	This work
NJ418	*unc-44* (+), *bli-6* (*sc16*)	Non-Unc Bli	This work
NJ413	*unc-44* (*rh1042*) *rev-1*2*	Sp. rev.	This work
Other *unc-44* mutants and revertants			
CB362	*unc-44* (*e362*)	Canonical allele	Brenner, 1974
SP1161	*dpy-13* (*e184*) *unc-44* (*q331*)	Sp. mut.	T. Schedl*
JK1040	*unc-44* (*q331, q332 rev*)	*q331* rev.	T. Schedl*
RW7220	*unc-44* (*st200*)	Sp. mut.	D. Moerman*
SP1167	*unc-44* (*st200, mn343 rev*)	*st200* rev.	W. Li*
SP1162	*unc-44* (*mn259*)	Sp. mut. from TR679	W. Li*
SP1164	*unc-44* (*mn259, mn340 rev*)	*mn259* rev.	W. Li*
SP1163	*unc-44* (*mn339*)	Sp. mut. from TR679	W. Li*
SP1166	*unc-44* (*mn339, mn342 rev*)	*mn339* rev.	W. Li*
Plasmids and bacteriophages			
DD#LRF7	λEMBL3 *unc-44* (*rh1042*): Tc*1*	12.6 kb EcoRI frag.	This work
DD#LRF1 to DD#LRF6	λEMBL3 *unc-44*	N2 partial Sau3aI	This work
BO350	pJB8 *unc-44* AmpR	N2 partial Sau3aI cosmid	This work‡
C44A	pJB8 *unc-44* AmpR	N2 partial Sau3aI cosmid	This work‡
DD#PPB40	pTZ18R *unc-44* AmpR	11 kb BO350 BamHI	This work
DD#PLT1840	pTZ18R *unr-44* AmpR	6 kb BO350 BamHI/SalI	This work
DD#PRF6	pTZ18R *unc-44* AmpR	5 kb BO350 BamHI/SalI	This work
DD#PRF7	pTZ18R *unc-44* AmpR	6 kb BO350 BamHI/SalI	This work
DD#PSLR8	pTZ18R *unc-44* AmpR	3.7 kb BO350 SalI	This work
DD#PAO13	pBluescript *unc-44* AmpR	N2 partial site B cDNA	This work§
DD#PAO49	pBluescript *unc-44* AmpR	N2 partial site A cDNA	This work§
DD#PAO66	pBluescript *unc-44* AmpR	N2 partial site A cDNA	This work§

The number of crosses to N2 is indicated after the allele number. For example, crossing of a strain containing the *rh1013* allele ten times to N2 would be indicated by *rh1013*10*.

* These mutations were isolated in the laboratories of J. Kimble, J. Shaw, R. Waterston, and R. Herman, and kindly provided by C. Kari and R. Herman.

‡ BO350 and C44A were kindly provided by A. Coulson and J. Sulston from their library (Coulson et al., 1986).

§ These cDNA clones were isolated from a bank provided by R. Barstead and R. Waterston (1989).

Mut., mutation; rev., revertant; sp., spontaneous.

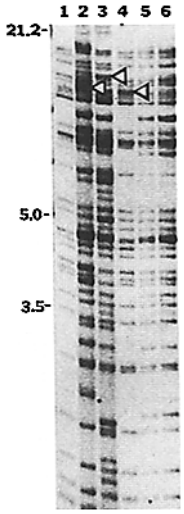

Figure 2. Southern blot analysis of the *unc-44 (rhl042)* allele. A Southern blot was prepared from EcoRI-digested DNA samples and probed with a Tc*1* plasmid. The samples are as follows: (lane *1*) wild-type N2; (lane *2*) NJ401 *unc-44 (rhl042)*; (lane *3*) NJ413 *unc-44 (rhl042) rev-1* revertant; (lane *4*) NJ416 *unc-44 (rhl042) bli-6 (scl6)* recombinant; (lane *5*) NJ417 *unc-44* (+) *bli-6 (scl6)* non-Unc, Blister recombinant; and (lane *6*) NJ418 *unc-44* (+) *bli-6 (sc-l6)*. Note the 12.6-kb fragment in the *unc-44* mutant strains (*arrows* in lanes *2* and *4*) and absence of this band in the other strains. In the case of a revertant, the 12.6-kb band is converted to a 14.2-kb band (*arrow* in lane *3*).

clones (DD#PAO49 and DD#PAO66) (Fig. 1 *b*). The carboxyl-terminal end of the large ankyrin isoform was obtained from cDNA clone DD#PAO13 (Fig. 1 *b*).

The ankyrin repeat, spectrin binding, and most of the conventional regulatory domains are arranged in 12 exons on clone DD#PPB40 (Figs. 1 *c* and 4). The 23 ankyrin repeats are grouped into six exons containing essentially 1, 5, 8½, 6, 1½, and 1 repeats (Figs. 1 *c* and 4). Introns cleanly separate exons that encode the first ankyrin repeat and the last ankyrin repeat, as is the case in vertebrate ankyrin (Tse, 1990). The clustering of repeat elements and the bifurcation of individual repeats is in contrast to the large number of single ankyrin repeat exons in the human *ANK1* gene (Tse, 1990).

Each individual repeat is more closely related to the corresponding repeat from other organisms than to the other nematode repeats (Fig. 5). The conservation of individual repeat sequences in organisms as divergent as humans and nematodes suggests a functional or structural role for each repeat. With the exception of a 7-aa insertion in repeat 5 of human brain ankyrin, the lengths of the corresponding nematode, mouse erythrocyte, human erythrocyte, and brain ankyrin repeats are identical. The constancy of the individual repeat lengths suggests stringent limits on the three-dimensional structure. The 7-aa insertion in the human brain ankyrin repeat 5 is not present in the *unc-44* genomic DNA, and therefore could not be obtained by simple alternative RNA splicing in the nematode. Repeats 2 through 6 and 8 through 12 contain the greatest number of identical residues (18 or more). There is 52% identity (396 of 755 residues) in the ankyrin repeat domains of the various ankyrins. The *unc-44* ankyrin repeat domain is more closely related to brain ankyrin (13% or 96 brain-specific residues, noted by asterisks in Fig. 5) than to erythrocyte ankyrin (5% or 39 erythrocyte-specific residues, noted by equal signs in Fig. 5). A number of residues are unique to the vertebrate ankyrin (13% or 101 residues, noted by periods in Fig. 5). The UNC-44 amino-terminal domain preceding the ankyrin repeats is also more similar in size and sequence to human brain ankyrin than to erythrocyte ankyrin (Fig. 5). These results suggest that the *unc-44* products are more closely related to the vertebrate brain ankyrin than to erythrocyte ankyrin.

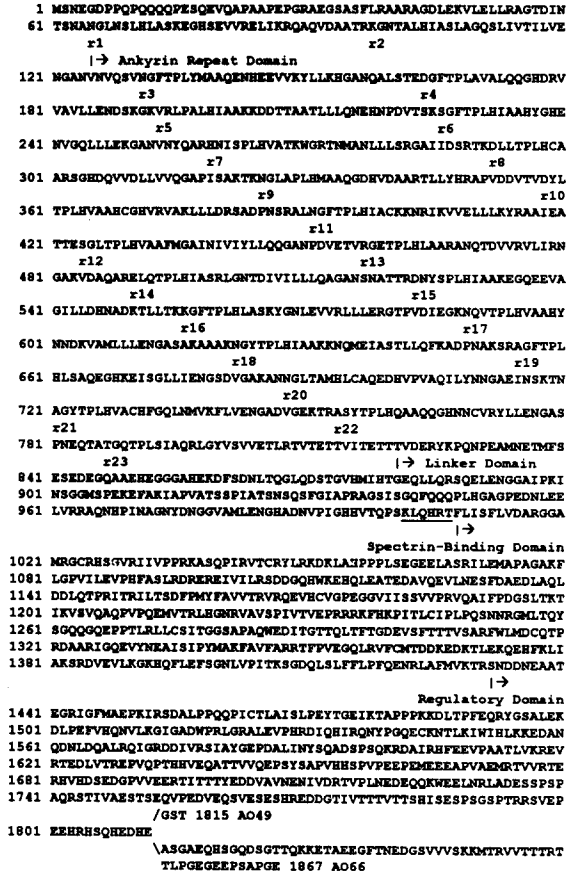

Figure 3. Predicted amino acid sequences of AO49 and AO66 ankyrin isoforms. The predicted protein sequences of AO49 and AO66 ankyrins are shown with the ankyrin repeats (r1–r23), linker, spectrin-binding, and regulatory domains noted. The alternatively spliced microexon present in AO49 ankyrin is underlined. At the bottom of the figure, the alternative carboxyl termini are noted. Amino acid residue positions are noted at the left margin.

unc-44 cDNA Fragments Encode Spectrin-binding and Regulatory Domains

DNA sequence analysis of DD#PAO49 and DD#PAO66 partial cDNA clones reveals linker, spectrin-binding, and regulatory domains (Fig. 6). The cDNA sequences are essentially identical in the central coding region with divergence at the 5′ and 3′ ends. The predicted protein fragments are hydrophilic and contain dispersed cysteine and proline residues. The open reading frame of DD#PAO49 includes a 6-aa alternatively spliced microexon adjacent to the strong spectrin-binding domain sequence similarity (Fig. 6). The divergence at the 5′ end of the DD#PAO66 cDNA is due to an inversion which is not detectable in the genome. The divergence at the 3′ end is due to alternative splicing, and leads to predicted full-length isoforms of 1815 aa (AO49 ankyrin, 198.8 kD) and 1867 aa (AO66 ankyrin, 204 kD) (Figs. 3 and 6).

The linker domain in *C. elegans* is larger (187 aa) than in human erythrocyte (113 aa) or brain (141 aa) ankyrins (Fig. 5). The linker domain contains the acidic portion of the spectrin-binding domain as defined by Davis and Bennett (1990), but has been separated in this report because the nematode sequence has considerably diverged from it, and

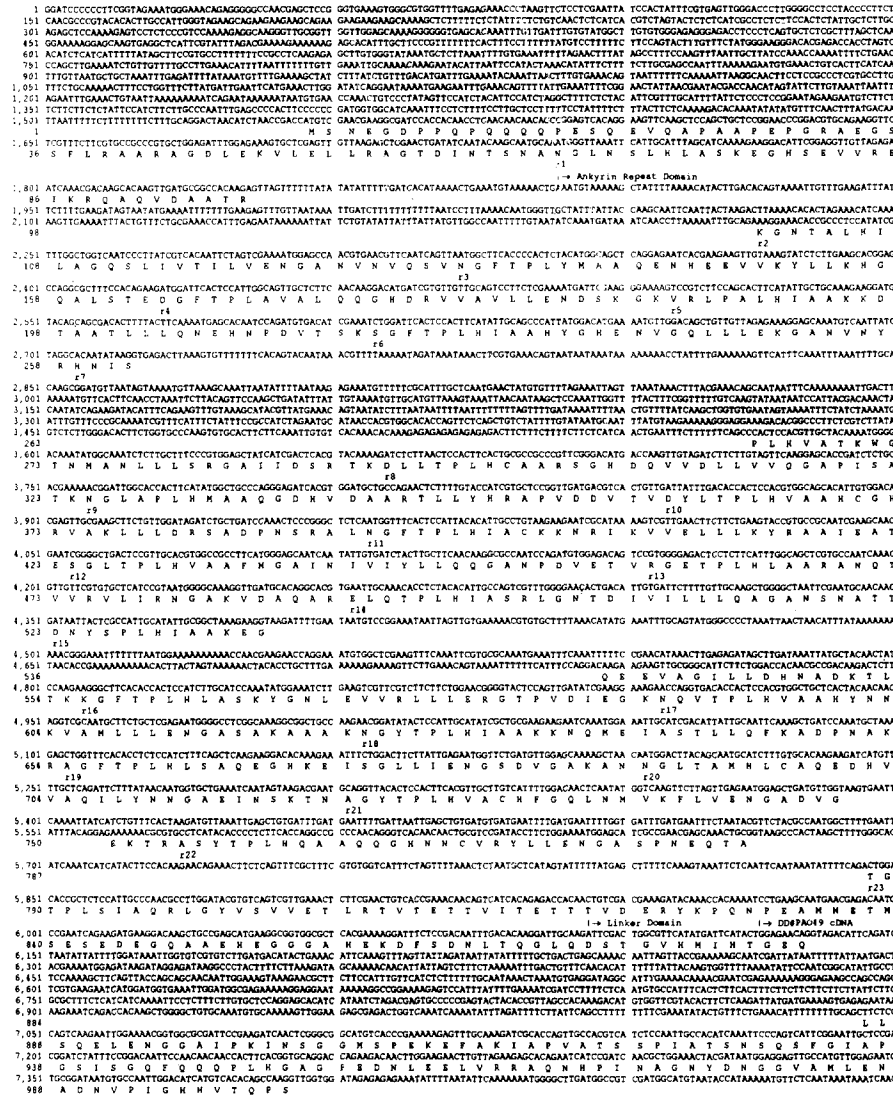

Figure 4. The nucleotide sequence of the 11-kb BamHI genomic DNA fragment. The nucleotide (nt) sequence of the 11-kb BamHI genomic fragment including the ankyrin repeat, linker, spectrin binding, and a portion of the regulatory domains is shown. The ankyrin repeats are noted below the protein sequence. The point of overlap with the DD#PAO49 cDNA clone is noted. Amino acid residue positions are noted at the left margin. These sequence data are available from EMBL/GenBank/DDBJ under accession number U21734.

it is not known whether the spectrin interaction with this region is specific (Davis and Bennett, 1990; Platt et al., 1993). The presence of the three introns in the linker domain could provide sequences for additional alternatively spliced exons. Searches of the intron sequences for vertebrate-like sequences failed to reveal cryptic exons.

A 47% protein sequence identity (198 residues) was found between brain, erythrocyte, and nematode ankyrins in the

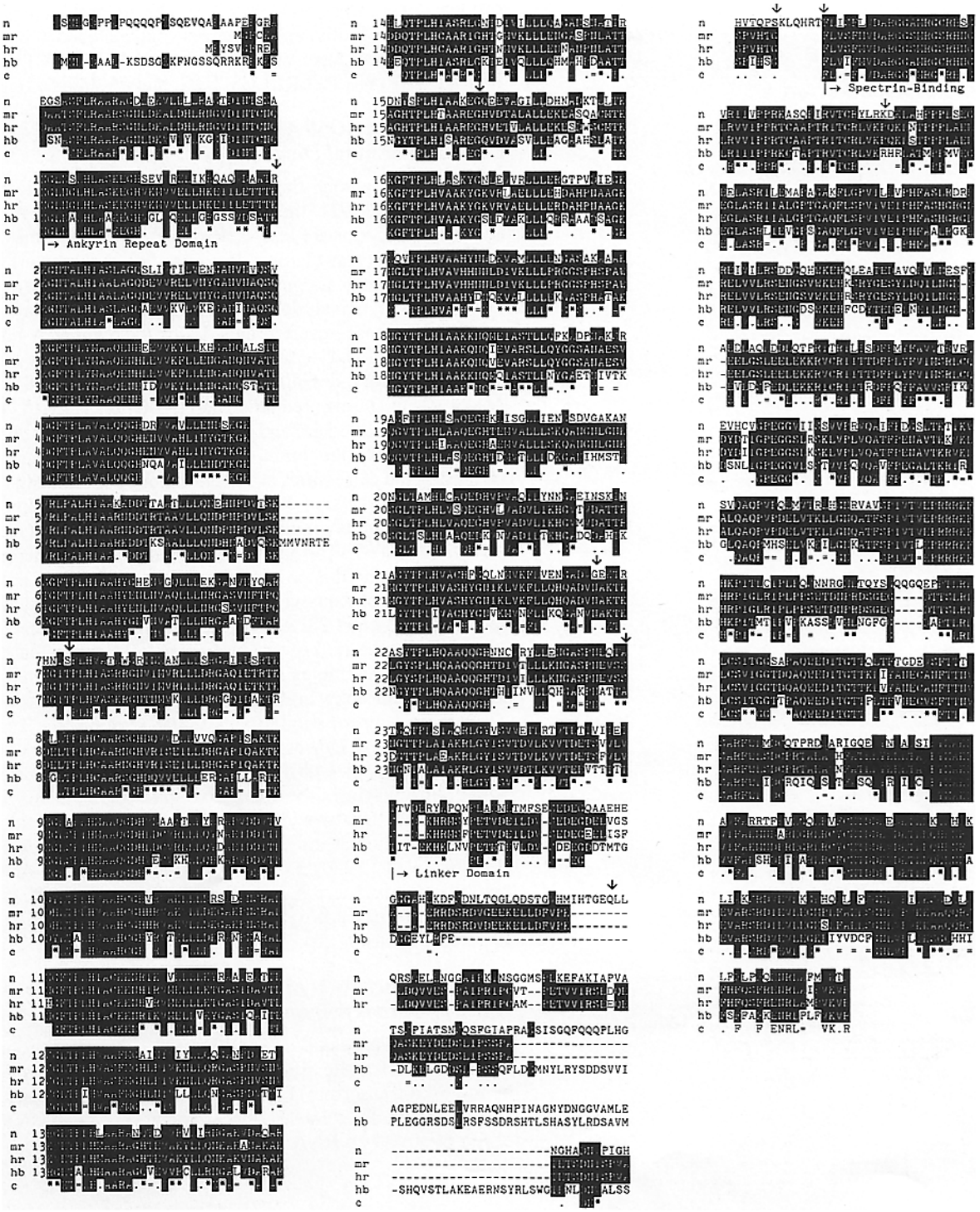

Figure 5. Comparison of the ankyrin repeat, linker, and spectrin-binding domains. The ankyrin repeat, linker, and spectrin-binding domains of nematode (n), mouse erythrocyte (mr) (White et al., 1992), human RBC (hr) (Lambert et al., 1990; Lux et al., 1990), and human brain (hb) (Otto et al., 1991) are compared. Identical residues are shown as inverse text. The consensus (c) sequence is shown below the various ankyrin sequences with brain-specific (*), erythrocyte-specific (=), and vertebrate-specific (.) residues noted. Ankyrin repeat numbers are listed at the left and the positions of introns in the nematode ankyrin are shown by the vertical arrows.

424–aa region of greatest spectrin-binding domain similarity (Fig. 5). The spectrin-binding domain similarity is intermediate between vertebrate brain and erythrocyte isoforms, suggesting that a single nematode gene may substitute for the multiple ankyrin genes in vertebrates. As with the ankyrin repeat domain, the spectrin-binding domain contains more brain-specific residues (12% or 50 residues) than erythrocyte-specific sequences (6% or 24 residues), and 18% (75

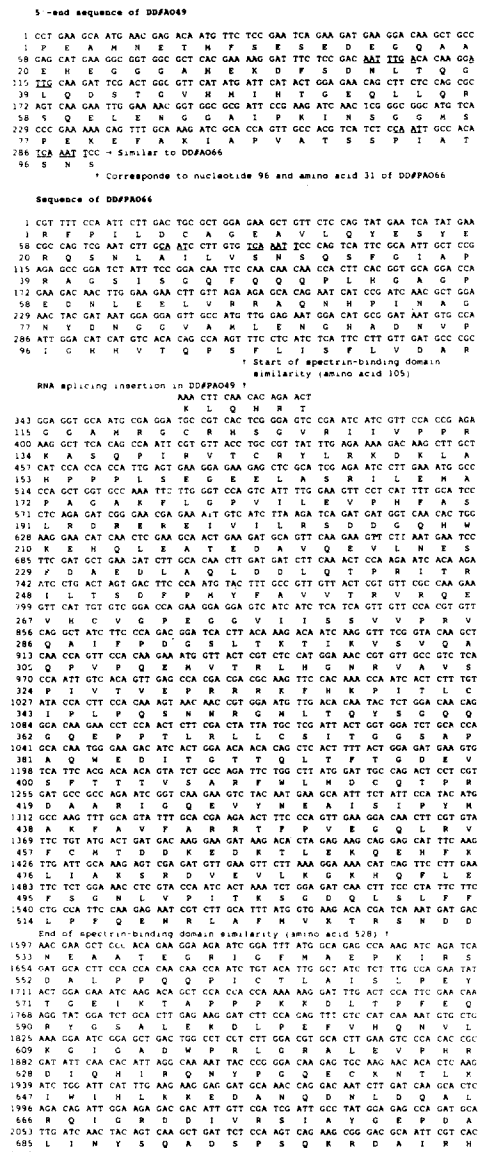

Figure 6. The AO49 and AO66 cDNA and predicted protein sequences. The DD#PAO49 sequence has been broken into three parts and aligned with the DD#PAO66 sequence. The 5′ end of DD#PAO49 joins the DD#PAO66 sequence at nt 97 (aa 31) just to the right of the DNA recombination site. The 18-nt insertion due to alternative splicing is shown below the DD#PAO66 sequence. The 3′ end of DD#PAO49 follows nt 2728 of DD#PAO66. The inverted repeat sequences at the breakpoints of the inversion near the 5′ end of the cDNAs (starting at nt positions 100 and 275 in DD#PAO49 and at position 74 in DD#PAO66) and a potential polyadenylation site (AATAAA) at the 3′ end of DD#PAO49 are underlined. A single nt difference at position 731 results in arginine 244 (AGA) being substituted by lysine (AAA) in DD#PAO49 and is assumed to be a cloning artifact. Potential hairpin structures near the 3′ ends of the cDNAs are noted by arrows. These sequence data are available from EMBL/GenBank/DDBJ under accession numbers U21731 and U21732.

residues) were vertebrate-specific. The longest nematode spectrin-binding domain sequences that matched the vertebrate sequences were VDARGGAMRGCRH, SPIVTVEPRRRKFHKPITL, PTLRLLCSITGG, and PAQWEDITGTT.

The AO49 and AO66 Ankyrin Carboxyl-terminal Domains

As is the case among the vertebrate conventional ankyrins (White et al., 1992), the regulatory domains of the AO49 and AO66 ankyrins are less well conserved than the ankyrin repeat and spectrin-binding domains. For this reason, the carboxyl-terminal assignments of sequence similarity are tentative. The nematode ankyrin regulatory domains are smaller than those in vertebrates. Using the regulatory binding domain boundary defined by Lux et al. (1990), the sizes of the regulatory domains are as follows: AO66, 381 aa; AO49, 324 aa; human red blood cell (RBC) 2.1 ankyrin, 497 aa; 2.2 ankyrin, 336 aa; and human brain ankyrin 2, 401 aa. Although weak, the amino acid sequence identities are greatest at the extremities of the regulatory domain (Fig. 7). Starting at aa position 1432 of full-length AO49 ankyrin, which marks the beginning of the predicted regulatory domain, a region of ~160 aa can be aligned with the vertebrate ankyrins. Beyond this point, neither AO49 nor AO66 ankyrins shows an obvious version of the band 2.1 exon that is spliced out in band 2.2 ankyrin. At position 1655, there is a short sequence in the vertebrate erythroid and nematode ankyrins that resembles a single copy of the 12-aa repeat found in brain ankyrin 1 (Otto et al., 1991). At position 1702, there is a poor similarity to a small region at the 3′ end of the "2.1 exon." Downstream of this sequence at position 1755 are two copies of a sequence that shares a similarity with brain ankyrin 1. The alternative splice in AO49 ankyrin near position 1810 provides an ending that is similar to the alternative splice at the very 3′ end of erythrocyte ankyrin (Lambert et al., 1990). Present at position 1815 of the AO66 ankyrin carboxyl terminus, but not in AO49 ankyrin, is a similarity to the carboxyl termini of the conventional vertebrate ankyrins.

DNA Sequence Analysis of the AO13 Ankyrin Carboxyl Terminus

The DNA sequence of DD#PAO13 reveals a potential protein fragment that is quite different from that putatively encoded by the 6-kb transcripts (Fig. 8). Northern blot analysis has shown that the DD#PAO13 cDNA clone corresponds to the 3′ end of a ~14-kb RNA. The deduced protein fragment is

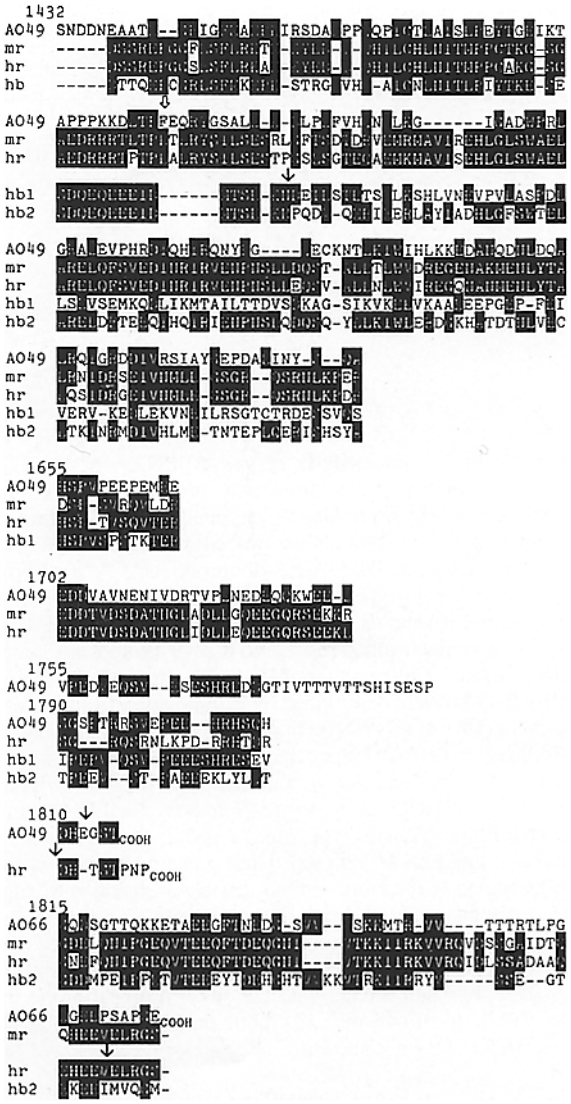

Figure 7. Comparison of ankyrin carboxyl-terminal domains. The carboxyl-terminal domains of nematode AO49, AO66, mouse erythrocyte (mr), human RBC (hr), human brain 1 (hbl), and human brain 2 (hb2) ankyrins are compared. Identical residues are presented as inverse text. The solid vertical arrows represent the positions of introns while the open arrow indicates the spectrin-binding/regulatory domain boundary (aa 1383) defined by Lux et al. (1990).

very acidic (predicted pI of 4.0). For this reason, searches of Entrez (release 11.0, June 1994) yielded the highest scores for acidic proteins, for example, the intermediate filament proteins. However, the structural characteristics found in the intermediate filament family of proteins (Steinert and Roop, 1988) are not obvious in the predicted protein product. The predicted AO13 ankyrin fragment contains a central 612–aa portion that is devoid of cysteine residues. The lack of cysteines (and therefore the possibility of disulfide cross-links in the central region), the hydrophilic character of the protein fragment, and the high predicted α-helical content suggest a filamentous structure. In addition to the acidic character of the deduced protein fragment, the most notable feature is a repeat of the sequence S(L/V) (T/S) SL (Q/A) EFERLEKE in the central portion (repeat A in Fig. 8). The transposon insertion in the *rhl042* allele is located between these repeats (Fig. 8). A shorter set of repeats containing the sequence TDSL occurs near the carboxyl terminus (repeat B in Fig. 8).

In the 3′ untranslated region of the cDNA, there are four inverted repeat sequences which may fold into hairpin structures in the mRNA. Three of the structures contain the sequence GCCCCAA in the loop of the hairpin.

Multiple Transcripts Encode Conventional and Large Ankyrins

Northern blot analysis revealed a major 6-kb band and several minor transcripts, including a ~14-kb transcript(s). To analyze the transcripts that arise from the 5′-half of the gene, probes from the AO49 spectrin-binding and regulatory domains were used (Fig. 9 *a*, lanes *1–6*). When blots of wild-type poly A–selected RNA (Fig. 9 *a*, lane *1*) or total RNA (Fig. 9 *a*, lane *2*) were probed, a major band at 5.95 ± 0.26 kb (n=79) was observed along with several less prevalent bands, including 3.19 ± 0.13 kb (n=45), 5.07 ± 0.10 kb (n=20), 6.91 ± 0.32 kb (n=32), and 13.86 ± 1.25 kb (n=8). Of particular interest is the wild-type ~14-kb minor transcript, near the limit of detection in Fig. 9 *a*, lanes *1* and *2*, and Fig. 9 *b*, lanes *1* and *2*. As detailed below, the ~14-kb transcript is the only transcript affected by all the insertion mutations, and therefore alterations in this transcript are responsible for the uncoordinated phenotype.

Besides the 5.95-kb, 6.91-kb, and 13.86-kb bands that were present in wild-type RNA, additional bands differing by the 1.6-kb size of Tc*1* were detected at 7.64 ± 0.28 kb (n=7), 8.55 ± 0.10 kb (n=4), and 14.79 ± 0.79 kb (n=9) in *rhl013* mutant RNAs (Fig. 9 *a*, lanes *3* and *4*). It appears that the transposon is transcribed into RNA, and somatic excision of the transposon gives rise to the normal sized RNAs in the mutants (Emmons and Yesner, 1984). In the *rhl042* mutant, the 5.07-, 5.95-, and 6.91-kb transcripts were unaffected by the downstream Tc*1* element (Fig. 9 *a*, lanes *5* and *6*). However, as in the *rhl013* mutant, the *rhl042* mutant RNA revealed the ~14-kb and ~15-kb bands. The ~15-kb band accumulates in the mutants to greater levels than the ~14-kb band, making it more readily detectable.

Transcripts overlapping the 3′-end of the gene were analyzed with DD#PAO13 riboprobe (Fig. 9 *a*, lanes *7–10*). The ~14-kb transcript was observed in wild-type RNA (Fig. 9 *a*, lanes *7* and *8*), and both ~14- and ~15-kb bands were found in the *rhl013* mutant (Fig. 9 *b*, lanes *9* and *10*).

The spanning of the entire gene by the ~14-kb RNA was demonstrated by probing blots of total RNA with the ankyrin repeat probe, stripping the blots, and reprobing the same blots with the DD#PAO13 riboprobe. Probing wild-type RNA with an ankyrin repeat probe (Fig. 9 *b*, lane *1*) revealed a weakly hybridizing ~14-kb band at exactly the same position as that obtained by reprobing with a DD#PAO13 probe (Fig. 9 *b*, lane *2*). Further evidence for a transcript that spans the entire gene is provided by analysis of the *rhl013* and *rhl042* mutant RNAs. Common bands at ~14 and ~15 kb were found in *rhl013* RNA with both probes (Fig. 9 *b*, lanes

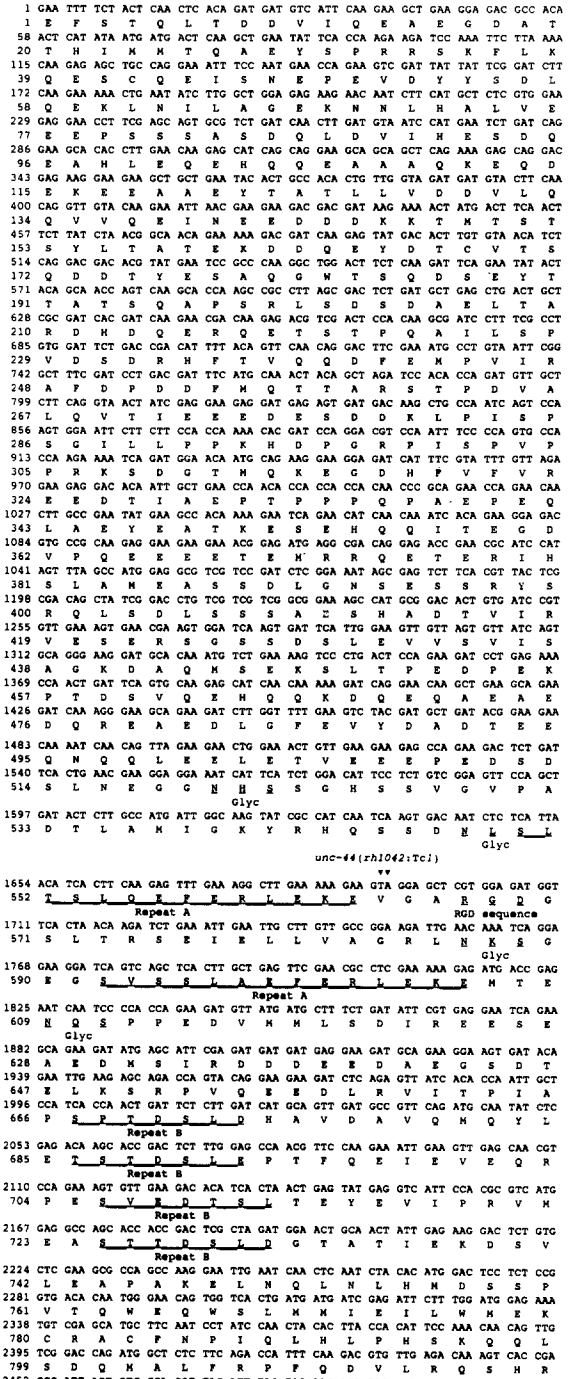

Figure 8. The predicted AO13 ankyrin carboxyl domain sequence. The nt and predicted aa sequences are presented as in Fig. 5. The uncertainty in the position of the Tc*1* element in the *rhl042* allele is due to the two-base-pair duplication created during Tc*1* insertion. The repeated motifs are noted by double underlines. Potential glycosylation sites (Glyc) and an RGD sequence (Singer et al., 1987) are noted by underlines. Potential hairpin structures are noted by arrows, and numbered, above the DNA sequences. Although the hairpin stems differ, three of the four loops contain the sequence GCCCCAA. Potential polyadenylation sequences, AATAAA, are underlined near the start of the polyadenylic acid tract at position 3340. These sequence data are available from EMBL/GenBank/DDBJ under accession number U21733.

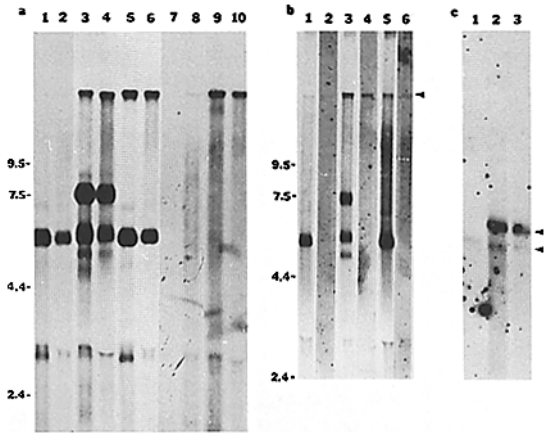

Figure 9. Northern blot analysis of *unc-44* RNAs. In panel *a*, Northern blots were prepared from poly A–selected RNA (*odd lanes*) or total RNA (*even lanes*) separated on a 1% agarose-formaldehyde gel. The blots were probed with an DD#PAO49 riboprobe (lanes *1–6*) or DD#PAO13 riboprobe (lane *7–10*). RNAs are as follows: N2 wild-type, lanes *1, 2, 7,* and *8*; *unc-44 (rhl013)*, lanes *3, 4, 9,* and *10*; and *unc-44 (rhl042)*, lanes *5* and *6*. The sizes of the RNAs were determined relative to 0.24–9.49-kb RNA markers (GIBCO-BRL, Gaithersburg, MD). The sizes of the RNAs larger than 9.49 kb were determined by extrapolation from the size marker curve (Otto et al., 1991). In panel *b*, common bands in the ~14–16-kb region (*arrow*) were detected by probing blots with the ankyrin repeat probe (*odd lanes*), and then reprobing the stripped blot with the DD#PAO13 riboprobe (*even lanes*). Total RNA samples are as follows: N2 wild-type, lanes *1* and *2*; *unc-44 (rhl013)*, lanes *3* and *4*; and *unc-44 (rhl042)*, lanes *5* and *6*. In panel *c*, the ~14–16-kb region of the Northern blot has been expanded by running the gel for an extended period of time. A ~14-kb band is present in wild-type RNA (lane *1*), while ~14- and ~15-kb bands (*arrows*) are present in RNAs from *unc-44 (q331)* (lane *2*) and *unc-44 (rhl013)* (lane *3*) when probed with the ankyrin repeat probe. In a manner similar to *rhl013*, the *q331* mutation affects several of the smaller mRNAs (data not shown).

3 and *4*), and also in *rhl042* mutant RNA (Fig. 9 *b*, lanes *5* and *6*).

To clearly distinguish the ~14- and ~15-kb RNAs (Fig. 9 *b*, *arrow*), wild-type and mutant RNAs were separated by extensive electrophoresis (Fig. 9 *c*). As can be clearly seen, wild-type RNA contains a ~14-kb band (Fig. 9 *c*, lane *1*), while both the ~14- and ~15-kb bands are present in the *q331* and *rhl013* mutants (Fig. 9 *c*, lanes *2* and *3*).

Discussion

In this paper, we report the molecular cloning of *unc-44*, a gene that is required for the correct targeting of axons to appropriate partners, and the identification of the putative gene

products as ankyrin-related proteins. Although the presence of ankyrin in the brain has been known for some time (Drenkhahn and Bennett, 1987), this paper provides the first evidence that ankyrins are required, directly or indirectly, for axonal guidance.

The following facts demonstrate that the *unc-44* gene has been definitively cloned. First, six *unc-44* mutations are due to DNA insertions. Four alleles (*mn259, q331, rh1013,* and *rh1042*) are Tc*1* insertions. The remaining two alleles (*mn339* and *st200*) are insertions that are larger than Tc*1*. Second, four revertants of *q331, rh1013,* and *mn259* are in-frame excisions of Tc*1*. Because in-frame excisions of Tc*1* are unusual, these results demonstrate that the restoration of the reading frame is critical for the function of the *unc-44* ankyrins. Third, complementation tests show that the DNA insertion mutations define a single complementation group, and that this complementation group corresponds to *unc-44*. Fourth, Northern blot and cDNA sequence analysis demonstrates that multiple transcripts are generated from *unc-44*, but that only the ~14-kb transcript(s) is affected by all the insertion alleles tested.

The isolation of several different cDNA clones demonstrated that the *unc-44* gene produces several alternatively spliced transcripts, with the most abundant RNA being ~6 kb. The ~6-kb RNA is smaller than the major vertebrate erythrocyte mRNAs which range from 6.8 to 9.5 kb (Lambert et al., 1990; Lux et al., 1990). However, the *unc-44* conventional ankyrins have smaller regulatory domains than the vertebrate proteins, which might account for part of the difference. The pattern of multiple mRNAs generated from *unc-44* (~3, 5, 6, 7, and 14 kb) is similar to the pattern of 4, 7, 9, and 13 kb RNAs from the neuronal *ANK-2* gene (Otto et al., 1991). The presence of alternatively spliced *unc-44* RNAs suggests that the products of this gene may play varied roles in the organism.

From the *unc-44* mutant phenotype, the complementation data, the RNA analysis, and the positions of the *unc-44* mutations, we propose that the large AO13 ankyrin is required for proper axonal guidance in *C. elegans*. The lack of cysteines in the central region of the AO13 ankyrin fragment and the predicted highly α-helical character of the domain suggest that the carboxyl-terminal domain has an extended structure. Exact repeats of the sequence EFERLEKE may indicate a functional role for these sequences.

This is the first demonstration that ankyrin plays a functional role in neural development. A role for AO13 ankyrin in neural development is reinforced by the finding that the 440-kD *ANK-2* product is present in the developing rat brain and is localized to neuronal processes (Kunimoto et al., 1991; Otto et al., 1991; Chan et al., 1993). Consequently, the predominant 6-kb *unc-44* messenger RNAs and the AO49 and AO66 ankyrins may not be critical for axon guidance.

Because the nematode *unc-44* ankyrin gene represents an evolutionarily primitive form, the conserved amino acid residues provide a starting point for structure-function analysis by site-directed mutagenesis and DNA transformation. The cloning and partial sequencing of the *unc-44* gene provides the foundation for molecular genetic analyses which may reveal specific roles for the various *unc-44* products in neurons and other cell types.

We thank the group of R. Herman for the kind gifts of the *unc-44* (mn259), *mn339, q331,* and *st200* mutants and revertants isolated in the laboratories of R. Herman, J. Kimble, J. Shaw, and R. Waterston; K. Nishiwaki and J. Miwa for the nematode genomic bank; R. Barstead, R. Waterston, I. Schauer, and W. Wood for cDNA banks; A. Coulson and J. Sulston for identifying and providing the cosmid clones; S. Emmons for the Tc*1* clone; J. Matsuzaki and S. Weldon for discussions; H. T. Cheung for his continued encouragement; W. Li for communication of unpublished results; H. T. Cheung and H. Brockman for critically reading the manuscript; and the Caenorhabditis Genetics Center for strains.

R. Franco was a National Institutes of Health postdoctoral trainee (grant T32-HDO-7299) for a one year period. This work was funded by gifts from TONEN, Inc., Saitama, Japan, a Biomedical Research Support Grant, Illinois State University Research Grants, and grants from the American Heart Association Illinois Affiliate and the National Science Foundation to A. J. Otsuka.

Portions of this work were previously presented in abstract form (Otsuka, A. J., R. Franco, B. Yang, K.-H. Shim, L. Z. Tang, A. Jeyaprakash, and P. Boontrakulpoontawee. 1991. *J. Cell Biol.* 115:465a. Abstr. 2706; Otsuka, A. J., P. Boontrakulpoontawee, Y.-Y. Zhang, L. Z. Tang, and A. Sobery. 1992. *Mol. Biol. Cell* 3:196a. Abstr. 1137; Boontrakulpoontawee, P., and A. J. Otsuka. 1993. *FASEB (Fed. Am. Soc. Exp. Biol.) J.* 7:A1079. Abstr. 159; Boontrakulpoontawee, P., and A. J. Otsuka. 1993. *Mol. Biol. Cell.* 4:571a. Abstr. 326; Boontrakulpoontawee, P., and A. J. Otsuka. 1994. *Mol. Biol. Cell.* 5:44a. Abstr. 255).

Received for publication 17 November 1994 and in revised form 28 February 1995.

References

Aviv, H., and P. Leder. 1972. Purification of biologically active globin messenger RNA by chromatography on oligothymidylic acid-cellulose. *Proc. Natl. Acad. Sci. USA.* 69:1408–1412.

Barstead, R. J., and R. H. Waterston. 1989. The basal component of the nematode dense-body is vinculin. *J. Biol. Chem.* 264:10177–10185.

Bennett, V. 1990. Spectrin-based membrane skeleton: a multipotential adaptor between plasma membrane and cytoplasm. *Physiol. Rev.* 70:1029–1065.

Bennett, V. 1992. Ankyrins: adaptors between diverse plasma membrane proteins and the cytoplasm. *J. Biol. Chem.* 267:8703–8706.

Brenner, S. 1974. The genetics of *Caenorhabditis elegans*. *Genetics.* 77:71–94.

Chan, W., E. Kordeli, and V. Bennett. 1993. 440-kD ankyrin$_B$: structure of the major developmentally regulated domain and selective localization in unmyelinated axons. *J. Cell Biol.* 123:1463–1473.

Collins, J., B. Saari, and P. Anderson. 1987. Activation of a transposable element in the germ line but not the soma of *Caenorhabditis elegans*. *Nature (Lond.).* 328:726–728.

Coulson, A., J. Sulston, S. Brenner, and J. Karn. 1986. Toward a physical map of the genome of the nematode *Caenorhabditis elegans*. *Proc. Natl. Acad. Sci. USA.* 83:7821–7825.

Davis, J., L. Davis, and V. Bennett. 1989. Diversity in membrane binding sites of ankyrins: brain ankyrin, erythrocyte ankyrin, and processed erythrocyte ankyrin associate with distinct sites in kidney microsomes. *J. Biol. Chem.* 264:6417–6426.

Davis, J. Q., T. McLaughlin, and V. Bennett. 1993. Ankyrin-binding proteins related to nervous system cell adhesion molecules: candidates to provide transmembrane and intracellular connections in adult brain. *J. Cell Biol.* 121:121–133.

Davis, L. H., and V. Bennett. 1990. Mapping the binding sites of human erythrocyte ankyrin for the anion exchanger and spectrin. *J. Biol. Chem.* 265: 10589–10596.

Davis, L. H., J. Q. Davis, and V. Bennett. 1992. Ankyrin regulation: an alternatively spliced segment of the regulatory domain functions as an intramolecular modulator. *J. Biol. Chem.* 267:18966–18972.

Dodd, J., and T. M. Jessell. 1988. Axon guidance and the patterning of neuronal projections in vertebrates. *Science (Wash. DC).* 242:692–699.

Drenckhahn, D., and V. Bennett. 1987. Polarized distribution of Mr 210,000 and 190,000 analogs of erythrocyte ankyrin along the plasma membrane of transporting epithelia, neurons and photoreceptors. *Eur. J. Cell Biol.* 43: 479–486.

Emmons, S. W., and L. Yesner. 1984. High-frequency excision of transposable element Tc*1* in the nematode *Caenorhabditis elegans* is limited to somatic cells. *Cell.* 36:599–605.

Georgatos, S. D., K. Weber, N. Geisler, and G. Blobel. 1987. Binding of two desmin derivatives to the plasma membrane and the nuclear envelope of avian erythrocytes: evidence for a conserved site-specificity in intermediate filament-membrane interactions. *Proc. Natl. Acad. Sci. USA.* 84:6780–6784.

Gumbiner, B. M. 1993. Proteins associated with the cytoplasmic surface of adhesion molecules. *Neuron.* 11:551–564.

Hall, T. G., and V. Bennett. 1987. Regulatory domains of erythrocyte ankyrin. *J. Biol. Chem.* 262:10537–10545.

Hedgecock, E. M., J. G. Culotti, and D. H. Hall. 1990. The *unc-5, unc-6,* and *unc-40* genes guide circumferential migrations of pioneer axons and mesodermal cells on the epidermis in *C. elegans. Neuron.* 2:61–85.

Hedgecock, E. M., J. G. Culotti, D. H. Hall, and B. D. Stern. 1987. Genetics of cell and axon migrations in *Caenorhabditis elegans. Development.* 100:365–382.

Hedgecock, E. M., J. G. Culotti, J. N. Thomson, and L. A. Perkins. 1985. Axonal guidance mutants of *Caenorhabditis elegans* identified by filling sensory neurons with fluorescein dyes. *Dev. Biol.* 111:158–170.

Henikoff, S. 1984. Unidirectional digestion with exonuclease III creates targeted breakpoints for DNA sequencing. *Gene (Amst.).* 28:351–359.

Jessell, T. M. 1988. Adhesion molecules and the hierarchy of neural development. *Neuron.* 1:3–13.

Kunimoto, M., E. Otto, and V. Bennett. 1991. A new 440-kD isoform is the major ankyrin in the neonatal rat brain. *J. Cell Biol.* 115:1319–1331.

Lambert, S., and V. Bennett. 1993. From anemia to cerebellar dysfunction – a review of the ankyrin gene family. *Eur. J. Biochem.* 211:1–6.

Lambert, S., H. Yu, J. T. Prchal, J. Lawler, P. Ruff, D. Speicher, M. C. Cheung, Y. W. Kan, and J. Palek. 1990. cDNA sequence for human erythrocyte ankyrin. *Proc. Natl. Acad. Sci. USA.* 87:1730–1734.

Lazarides, E., and C. Woods. 1989. Biogenesis of the red blood cell membrane skeleton and the control of erythroid morphogenesis. *Annu. Rev. Cell Biol.* 5:427–452.

Lehrach, H., D. Diamond, J. M. Wozney, and H. Boedtker. 1977. RNA molecular weight determinations by gel electrophoresis under denaturing conditions, a critical reexamination. *Biochemistry.* 16:4743–4751.

Leung-Hagesteijn, C., A. M. Spence, B. D. Stern, Y. Zhou, M.-W. Su, E. M. Hedgecock, and J. G. Culotti. 1992. UNC-5, a transmembrane protein with immunoglobulin and thrombospondin type 1 domains, guides cell and pioneer axon migrations in *C. elegans. Cell.* 71:289–299.

Lux, S. E., K. M. John, and V. Bennett. 1990. Analysis of cDNA for human erythrocyte ankyrin indicates a repeated structure with homology to tissue-differentiation and cell-cycle control proteins. *Nature (Lond.).* 344:36–42.

MacLeod, A. R., J. Karn, and S. Brenner. 1981. Molecular analysis of the *unc-54* myosin heavy-chain gene of *Caenorhabditis elegans. Nature (Lond.).* 291:386–390.

Maniatis, T., E. F. Fritsch, and J. Sambrook. 1982. Molecular Cloning: A Laboratory Manual. Cold Spring Harbor Laboratory, Cold Spring Harbor, New York.

McIntire, S. L., G. Garriga, J. White, D. Jacobson, and H. R. Horvitz. 1992. Genes necessary for directed axonal elongation or fasciculation in *C. elegans. Neuron.* 8:307–322.

Michaely, P., and V. Bennett. 1992. The ANK repeat: a ubiquitous motif involved in macromolecular recognition. *Trends Cell Biol.* 2:127–129.

Mori, I., D. G. Moerman, and R. H. Waterston. 1988. Analysis of a mutator activity necessary for germline transposition and excision of Tc*1* transposable elements in *Caenorhabditis elegans. Genetics.* 120:397–407.

Mount, S. M., M. M. Green, and G. M. Rubin. 1988. Partial revertants of the transposable element-associated suppressible allele *white-apricot* in *Drosophila melanogaster*: structures and responsiveness to genetic modifiers. *Genetics.* 118:221–224.

Otsuka, A. J., V. I. Wheaton, and E. Hedgecock. 1987. Transposon tagging of genes affecting axonal outgrowth in *Caenorhabditis elegans. UCLA Symp. Mol. Cell. Biol.* 51:665–671.

Otto, E., M. Kunimoto, T. McLaughlin, and V. Bennett. 1991. Isolation and characterization of cDNAs encoding human brain ankyrins reveal a family of alternatively spliced genes. *J. Cell Biol.* 114:241–253.

Peters, L. L., and S. E. Lux. 1993. Ankyrins: structure and function in normal cells and hereditary spherocytes. *Semin. Hematol.* 30:85–118.

Platt, O. S., S. E. Lux, and J. F. Falcone. 1993. A highly conserved region of human erythrocyte ankyrin contains the capacity to bind spectrin. *J. Biol. Chem.* 268:24421–24426.

Rathjen, F. G., U. Norenberg, and H. Volkmer. 1992. Glycoproteins implicated in neural cell adhesion and axonal growth. *Biochem. Soc. Trans.* 20:405–409.

Sanes, J. R. 1989. Extracellular matrix molecules that influence neural development. *Annu. Rev. Neurosci.* 12:491–516.

Sanger, F., S. Nicklen, and A. R. Coulson. 1977. DNA sequencing with chain-terminating inhibitors. *Proc. Natl. Acad. Sci. USA.* 74:5463–5467.

Serafini, T., T. E. Kennedy, M. J. Galko, C. Mirzayan, T. M. Jessell, and M. Tessier-Lavigne. 1994. The netrins define a family of axon outgrowth-promoting proteins homologous to *C. elegans* UNC-6. *Cell.* 78:409–424.

Siddiqui, S. S. 1990. Mutations affecting axonal growth and guidance of motor neurons and mechanosensory neurons in the nematode *Caenorhabditis elegans. Neurosci. Res. (Suppl.).* 13:171–190.

Siddiqui, S. S., and J. G. Culotti. 1991. Examination of neurons in wild type and mutants of *Caenorhabditis elegans* using antibodies to horseradish peroxidase. *J. Neurogenetics.* 7:193–211.

Singer, I. I., D. W. Kawka, S. Scott, R. A. Mumford, and M. W. Lark. 1987. The fibronectin cell attachment sequence arg-gly-asp-ser promotes focal contact formation during early fibroblast attachment and spreading. *J. Cell Biol.* 104:573–584.

Steinert, P. M., and D. R. Roop. 1988. Molecular and cellular biology of intermediate filaments. *Annu. Rev. Biochem.* 57:593–625.

Sulston, J. E., and S. Brenner. 1974. The DNA of *Caenorhabditis elegans. Genetics.* 77:95–104.

Takeichi, M. 1988. The cadherins: cell-cell adhesion molecules controlling animal morphogenesis. *Development.* 102:639–655.

Takeichi, M. 1991. Cadherin cell adhesion receptors as a morphogenetic regulator. *Science (Wash. DC).* 251:1451–1455.

Tse, W. T. 1990. A molecular analysis of the spectrin and ankyrin genes in normal and abnormal red blood cells. Ph. D. thesis. Yale University, New Haven, CT. pp. 1–191.

Wadsworth, W. G., and E. M. Hedgecock. 1992. Guidance of neuroblast migrations and axonal projections in *Caenorhabditis elegans. Curr. Opin. Neurobiol.* 2:36–41.

Wallin, R., E. N. Culp, D. B. Coleman, and S. R. Goodman. 1984. A structural model of human erythrocyte band 2.1: alignment of chemical and functional domains. *Proc. Natl. Acad. Sci. USA.* 81:4095–4099.

Weaver, D. C., and V. T. Marchesi. 1984. The structural basis of ankyrin function: I. Identification of two structural domains. *J. Biol. Chem.* 259:6165–6169.

Weaver, D. C., G. R. Pasternack, and V. T. Marchesi. 1984. The structural basis of ankyrin function: II. Identification of two functional domains. *J. Biol. Chem.* 259:6170–6175.

White, J. G., E. Southgate, J. N. Thomson, and S. Brenner. 1986. The structure of the nervous system of the nematode *Caenorhabditis elegans. Phil. Trans. Roy. Soc. Lond.* 314:1–340.

White, R. A., C. S. Birkenmeier, L. L. Peters, J. E. Barker, and S. E. Lux. 1992. Murine erythrocyte ankyrin cDNA: highly conserved regions of the regulatory domain. *Mamm. Genome.* 3:281–285.